SwarmThinkers: Learning Physically Consistent **Atomic KMC Transitions at Scale**

Oi Li*

University of Science and Technology of China

Kun Li[†]

Microsoft Research

Haozhi Han

Peking University

Honghui Shang

University of Science and Technology of China

Xinfu He

China Institute of Atomic Energy

Yunguan Zhang

Chinese Academy of Sciences

Hong An

University of Science and Technology of China

Ting Cao

Microsoft Research

Mao Yang

Microsoft Research

Abstract

Can a scientific simulation system be physically consistent, interpretable by design, and scalable across regimes—all at once? Despite decades of progress, this trifecta remains elusive. Classical methods like Kinetic Monte Carlo ensure thermodynamic accuracy but scale poorly; learning-based methods offer efficiency but often sacrifice physical consistency and interpretability. We present **SwarmThinkers**, a reinforcement learning framework that recasts atomic-scale simulation as a physically grounded swarm intelligence system. Each diffusing particle is modeled as a local decision-making agent that selects transitions via a shared policy network trained under thermodynamic constraints. A reweighting mechanism fuses learned preferences with transition rates, preserving statistical fidelity while enabling interpretable, step-wise decision making. Training follows a centralized-training, decentralized-execution paradigm, allowing the policy to generalize across system sizes, concentrations, and temperatures without retraining. On a benchmark simulating radiation-induced Fe-Cu alloy precipitation, SwarmThinkers is the first system to achieve full-scale, physically consistent simulation on a single A100 GPU—previously attainable only via OpenKMC on a supercomputer. It delivers up to 4,963× (3,185× on average) faster computation with 485× lower memory usage. By treating particles as decision-makers—not passive samplers—SwarmThinkers marks a paradigm shift in scientific simulation: one that unifies physical consistency, interpretability, and scalability through agent-driven intelligence.

Introduction

Scientific simulation serves as a cornerstone of modern science, enabling insight and prediction across fields—from radiation damage to catalysis to phase transformations [1, 2, 3, 4, 5, 6]. Among these, Kinetic Monte Carlo [7, 8, 9] stands out for modeling rare-event dynamics over extended timescales, grounded in physically derived transition rates [10, 11, 12].

^{*}Work done during an internship at Microsoft Research (in 2024.6),

[†]Corresponding author: Kun Li (likungw@gmail.com)

However, classical KMC is fundamentally **passive**: transitions are sampled blindly from predefined rates, treating all events as equally probable regardless of their downstream impact. In realistic systems, only a small subset of transitions meaningfully shape long-term structure [13, 14, 15, 16, 17]. As a result, simulations waste vast compute resolving reversible fluctuations while missing opportunities to prioritize structure-forming transitions. Existing advances such as event cataloging [18, 19, 20, 21], rejection-free methods [22, 23, 24, 25], and neural surrogates [26, 27] retain this sampling-centric paradigm, often at the cost of scalability, interpretability, or physical consistency.

This raises a deeper question: *Can particles in simulation learn to think?* That is, can we move beyond passive sampling, toward systems where particles make physically grounded, structure-aware, and goal-directed decisions to drive long-term evolution?

We propose **SwarmThinkers**, a new reinforcement learning framework that reimagines atomic-scale simulation as a *physically constrained swarm intelligence system*. Each diffusing particle is modeled as an autonomous agent that perceives its local context and selects transitions via a shared policy network. Rather than sampling independently, all agent-direction pairs are pooled into a unified global softmax, allowing the system to prioritize kinetically meaningful events in a coordinated, structure-aware manner. To preserve physical consistency, we introduce a *reweighting mechanism* that fuses policy-driven preferences with classical transition rates, and apply *trajectory-level importance sampling* to ensure unbiased estimation of physical observables and statistics. Physical knowledge is deeply embedded: action constraints reflect local bonding physics, rewards capture thermodynamic relaxation, and critics encode global structure. Training follows a centralized-training, decentralized-execution (CTDE) paradigm, enabling generalization across system sizes, concentrations, and temperature regimes.

As summarized in Table 1, SwarmThinkers uniquely achieves state-of-the-art performance across all metrics: 3,185x faster simulation, 6.68×10^{-2} transition energy per step, and 0.34 effective transition ratio. For the first time, a single GPU scales over 54 billion atoms using less than 60GB of memory, matching the fidelity of previous supercomputer-scale simulations that required over five million cores. From supercomputers to a single GPU, from passive sampling to active reasoning, from scale-bound heuristics to generalizable intelligence—SwarmThinkers represents a paradigm shift toward scalable, physically grounded, agent-driven scientific systems.

Table 1: Comparison of SwarmThinkers and KMC Acceleration Strategies. Metrics include Spd (Speedup over OpenKMC), TPE (Transition Per-step Energy), and ETR (Effective Transition Ratio). Scale evaluates billion-atom scalability; CF indicates fidelity in cluster formation; Gen. assesses generalization across diverse simulation regimes, including different system sizes, temperatures, and Cu/vacancy concentrations.

Cat.	Method	Spd (↑)	TPE (eV , ↑)	ETR (↑)	Scale	CF	Gen.
Classic	OpenKMC [28]	1.00x	$< 10^{-5}$	$ < 10^{-4}$	✓	1	✓
ML-Surr. ML-Surr.	MC-PINNs [26] NNP-KMC [27]	1.00x 1.00x	$< 10^{-5} < 10^{-5}$	$ < 10^{-4} < 10^{-4}$	X X	X ✓	✓ ×
Biased Biased Biased Biased	hyper-MD [29] SpecTAD [30] PS-KM [31] tRPS [32]	15.13x 15.86x 62.52x 77.63x	3.19×10^{-4} 3.25×10^{-4} 1.32×10^{-3} 1.65×10^{-3}		X X X	\ \ \ \ \ \ \ \ \	\ \ \ \
RL-based RL-based	TKS-KMC [33] PGMC [34]	1783.18x 2652.54x	$4.16 \times 10^{-2} \\ 5.71 \times 10^{-2}$	0.21 0.26	X X	√ ✓	X X
Ours	SwarmThinkers	3185.40x	$6.86 imes 10^{-2}$	0.34	/	1	1

2 Related Work

2.1 Classical KMC

Kinetic Monte Carlo models thermally activated processes such as diffusion [35, 36, 37, 38], defect clustering [39, 40], and irradiation damage by sampling transitions from physically derived rate

laws [28, 41, 42]. However, classical KMC remains fundamentally passive: all transitions are sampled solely based on local energy barriers, with no memory, prioritization, or structural feedback. This yields statistically valid but behaviorally unintelligent simulations—unable to focus compute on impactful events or adapt to evolving system dynamics.

2.2 HPC-Accelerated KMC

To address computational inefficiency, various acceleration techniques have been proposed. Hyperdynamics [29, 43, 44] and parallel replica methods [45, 46, 47] increase event frequency via bias potentials or replica averaging, while adaptive KMC frameworks reduce transition search costs through on-the-fly catalog generation [48, 49, 8]. System-level efforts such as OpenKMC [28], SPPARKS [50], and TensorKMC [51] scale to billions of atoms by exploiting massive parallelism. Yet these methods preserve the same core limitation: transition selection remains context-free and rate-based, lacking awareness of system structure or long-term objectives.

2.3 Learning-Augmented KMC

Machine learning has been introduced to enhance adaptability and reduce cost. Surrogate models predict transition rates from atomic configurations [52, 53, 26, 27], graph neural networks encode structural priors [54, 55, 56], and reinforcement learning has been used to guide transition selection [33, 34]. Despite these advances, key challenges remain: surrogates often break thermodynamic fidelity, centralized RL fails to generalize to large systems, and most models function as black boxes, limiting scientific interpretability and integration.

3 Why Scaling Simulation Is Not Enough: Toward Intelligent Physical Modeling

3.1 The Brute-Force Ceiling: OpenKMC at Supercomputer Scale

One of the most critical and computationally demanding challenges in materials simulation is modeling the thermal aging of Fe-Cu alloys in reactor pressure vessel (RPV) steels—a canonical system in nuclear materials science [57, 58, 59, 60]. Over decades of in-service time, nanoscale Cu clusters nucleate and grow, driving embrittlement. Capturing this long-timescale evolution requires simulating billions of atoms over hundreds of years of rare-event dynamics [60, 58, 61, 62, 63].

To date, the only system capable of achieving this is **OpenKMC**, a massively parallel kinetic Monte Carlo framework that runs on a supercomputer. It successfully reproduces long-timescale Cu precipitation in bcc lattices, with results that match experimental observations in both kinetics and morphology. This marks a milestone: the first atomistic simulation of a full-scale nuclear material system with over 100 billion atoms [28].

However, this success also exposes the limitations of the underlying paradigm. OpenKMC, like all KMC variants, relies on passive sampling: transitions are selected from rate laws without foresight, feedback, or global coordination. Its scaling stems from raw computational power, not algorithmic intelligence. As systems grow larger and longer in timescale, this brute-force approach encounters a ceiling: *scaling computation alone cannot substitute for scalable intelligence*.

3.2 What's Missing: Temporal, Spatial, and Strategic Intelligence

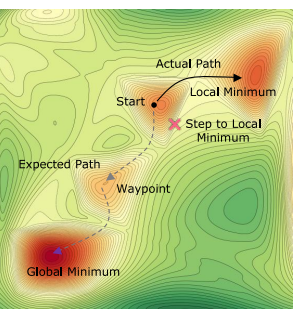
To break through this ceiling, scientific simulation must evolve beyond passive sampling, toward intelligent, structure-aware reasoning. We identify three core capabilities that current simulation paradigms lack:

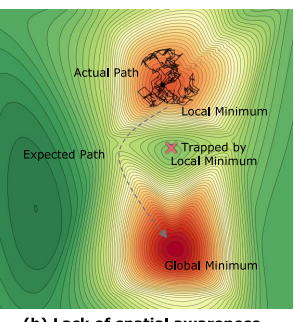
Temporal reasoning. The ability to plan across steps—to foresee multi-hop pathways or delayed rewards, and avoid shortsighted decisions that trap systems in suboptimal states.

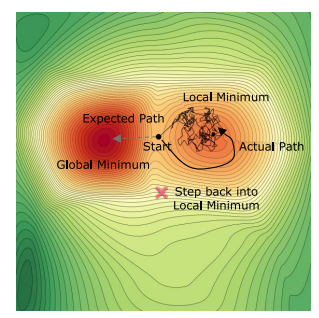
Spatial awareness. The ability to act in context—understanding defect fields, long-range correlations, and global structure when choosing transitions, rather than sampling myopically.

Strategic adaptivity. The ability to learn from failure—suppressing unproductive transitions, reusing successful pathways, and dynamically allocating attention where change matters most.

These capabilities remain absent in existing paradigms, which is illustrated in Figure 1. Passive sampling frameworks, even when massively scaled, treat every event in isolation. What's needed is a simulation system that integrates *local decision-making with global physical constraints*—where particles no longer merely react, but begin to act with purpose.







(a) Lack of temporal reasoning

(b) Lack of spatial awareness

(c) Lack of strategic adaptivity

Figure 1: Illustration of key limitations in conventional KMC paradigms. (a) Lack of temporal reasoning: short-sighted transitions lead to early trapping in local minima, missing delayed but critical structural pathways. (b) Lack of spatial awareness: local decisions ignore global structure, causing the system to wander within energetically unfavorable basins. (c) Lack of strategic adaptivity: Even when near the global minimum, the system may revert to previously explored local minima, failing to suppress historically unproductive transitions.

4 Method

4.1 Preliminary: Kinetic Monte Carlo Method

To ground our framework, we first review the classical Kinetic Monte Carlo formulation widely used for simulating long-timescale dynamics in crystalline solids. In body-centered cubic (bcc) systems such as Fe–Cu alloys, diffusion proceeds via vacancy-mediated hops, where a vacancy exchanges positions with one of its neighboring atoms. The transition rate of a vacancy-atom hop event X follows the Arrhenius form:

$$\Gamma_X = \Gamma_0 \exp\left(-\frac{E_a^X}{kT}\right), \quad E_a^X = E_a^0 + \frac{1}{2}(E_f - E_i),$$
 (1)

where Γ_0 is the attempt frequency, k the Boltzmann constant, and T the temperature. E_a^0 is a species-specific reference barrier, and E_i, E_f are system energies before and after the hop. These energies are evaluated using a chemically resolved pairwise potential:

$$E_{\text{pair}} = \sum_{i} n_i \varepsilon_{\text{type}}^{(i)}, \tag{2}$$

where n_i is the number of bonds of type type in the *i*-th neighbor shell, and $\varepsilon_{\text{type}}^{(i)}$ the corresponding bond energy. This local model captures short-range chemical effects in dilute alloys.

Given the full set of transition rates $\{\Gamma_X\}$, the system evolves using the residence-time algorithm. At each step, an event is selected according to:

$$\Gamma_{\text{tot}} = \sum_{X} \Gamma_{X}, \quad \mathbb{P}(X) = \frac{\Gamma_{X}}{\Gamma_{\text{tot}}},$$
(3)

and the time increment is sampled as:

$$\Delta t = -\frac{\ln r}{\Gamma_{\text{tot}}}, \quad r \sim \mathcal{U}(0, 1), \tag{4}$$

where r is re-sampled at each KMC step to reflect stochastic evolution.

4.2 Particles That Think: Learning to Prioritize Transitions

We design a reinforcement learning framework with four key components, which enable atomic-scale agents to prioritize kinetically significant transitions while preserving alignment with first-principles physics.

Local Observation. Each agent i encodes its atomic environment by observing a fixed-radius neighborhood \mathcal{N}_i consisting of first- and second-nearest neighbors. This domain-informed locality reflects the short-range nature of interatomic interactions, where transition barriers are determined primarily by discrete species configurations rather than geometric coordinates.

We represent the neighborhood as a fixed-length vector:

$$o_i = [\sigma_{ij}]_{j \in \mathcal{N}_i}, \quad o_i \in \mathbb{R}^n,$$

where $\sigma_{ij} \in \mathbb{Z}$ denotes the atomic species of neighbor j, and $n = |\mathcal{N}_i|$ is the total number of neighbors. This minimalist, symmetry-aware encoding provides a lightweight yet physically grounded state representation.

Importantly, this discrete, topology-preserving encoding captures all transition-relevant factors while abstracting away global details, yielding an input space invariant to system size, defect density, and geometry. It thus provides a scalable foundation for structure-aware decision-making across domains.

Decentralized Policy. To reflect the global event selection nature of KMC, we adopt a decentralized policy where each diffusing agent proposes local transitions that are jointly prioritized at the system level. This design decouples local representation from global selection: each agent encodes its neighborhood $o_i \in \mathbb{R}^d$ via an MLP to produce directional logits:

$$z_i = f_{\theta}(o_i), \quad z_i \in \mathbb{R}^K,$$
 (5)

The final decision emerges from a global coordination process. Specifically, all agent-direction logits are flattened into a single vector:

$$z = \operatorname{concat}(z_1, z_2, \dots, z_N), \quad z \in \mathbb{R}^{NK}, \tag{6}$$

and passed through a softmax to yield a joint distribution over the entire candidate set:

$$\pi_{\theta}(a \mid o_{1:N}) = \frac{\exp(z_a)}{\sum_{a'=1}^{NK} \exp(z_{a'})}, \quad a \in \{1, \dots, NK\}.$$
 (7)

The global softmax serves as a differentiable arbitration layer, enabling direct competition among all agent-proposed transitions while retaining localized representations. This fosters swarm-level structural awareness, allowing globally significant transitions to dominate even among locally similar candidates. Its differentiability supports end-to-end training guided by long-horizon structural objectives. Crucially, the learned policy π_{θ} is not executed directly, but modulated by physical rates to preserve thermodynamic consistency (see Sec . 4.3). This separation of intent and execution enables intelligent yet physically valid sampling.

Centralized Critic. To complement the local policy, we introduce a centralized value function $V_{\phi}(s)$ for system-level credit assignment. The input is constructed as $s = \operatorname{concat}(s_{\text{obs}}, s_{\text{stat}})$, where

$$s_{\text{obs}} = \text{concat}(o_1, \dots, o_N), \quad s_{\text{stat}} = \text{concat}(\boldsymbol{\mu}, \boldsymbol{\sigma}, c, d, \rho).$$
 (8)

Here, $\mu, \sigma \in \mathbb{R}^3$ are the spatial mean and variance of Cu positions; c, d, and $\rho \in \mathbb{R}$ represent local Cu density heterogeneity, average vacancy—Cu distance, and Cu clustering around vacancies, respectively. These descriptors capture key mesoscopic features linked to phase separation, aggregation, and long-range defect interactions. By fusing microscopic observations with coarse-grained statistics, the critic enables scale-bridging credit assignment, linking short-term transitions to long-term structural outcomes. The value function is implemented as a multilayer perceptron:

$$v = f_{\phi}(s), \quad v \in \mathbb{R},$$
 (9)

and produces a scalar used to compute advantage estimates during policy optimization.

This globally informed signal enhances the policy's ability to discern kinetically meaningful transitions, reduces variance in training across heterogeneous spatial configurations, and stabilizes credit assignment in large-scale systems.

Reward and Training. We adopt a CTDE framework for scalable, structure-aware learning. Agents receive only local observations o_i , while the critic leverages global context to assign long-range credit, enabling localized execution with system-level feedback. The reward is defined as the negative change in total system energy:

$$r_t = -\Delta E_t, \quad \Delta E_t = E_{t+1} - E_t, \tag{10}$$

where E_t denotes the system energy at time step t. This physics-grounded minimalist reward reflects the thermodynamic drive toward lower-energy states, guiding the policy to discover transition sequences that accelerate structural relaxation. Crucially, we avoid task-specific shaping, preserving fidelity to the underlying physics and allowing the system to infer meaningful dynamics from first principles.

We optimize the policy using proximal policy optimization (PPO), with advantage targets derived from the centralized critic. By combining local proposals via a global softmax and evaluating outcomes through structure-aware value estimates, the framework enables *delayed credit assignment*—linking long-term morphological changes to earlier local transitions.

This architecture enables strong generalization: since agents rely solely on local observations and actions, the learned policy is invariant to system size, geometry, and defect morphology. Models trained on small domains can thus be deployed directly to large, heterogeneous systems, supporting fast, physically consistent simulation across scales.

4.3 Embedding Thermodynamics: Preserving Statistical Consistency

While the learned policy $\pi_{\theta}(a \mid o_{1:N})$ encodes structural preferences that accelerate transitions, physical fidelity must be preserved. Classical KMC transitions are sampled strictly according to Eq. 3. Replacing this with a purely learned distribution would violate real-time dynamics.

Reweighted Sampling Formulation. To reconcile structure-aware prioritization with thermodynamic correctness, we construct a reweighted distribution over all agent-direction pairs $a \in \mathcal{A}$:

$$P(a) = \frac{\pi_{\theta}(a \mid o_{1:N}) \cdot \Gamma_a}{\sum_{a'} \pi_{\theta}(a' \mid o_{1:N}) \cdot \Gamma_{a'}},\tag{11}$$

The hybrid $P(a) \propto \pi_{\theta}(a) \Gamma_a$ enhances sampling efficiency but deviates from the physical distribution. We correct this bias via *Importance Sampling* to ensure statistical consistency.

Unbiased Estimation. Let p(a) denote the original KMC distribution and q(a) the policy-modulated proposal:

$$p(a) = \frac{\Gamma_a}{\sum_{a'} \Gamma_{a'}}, \quad q(a) = \frac{\pi_\theta(a) \Gamma_a}{\sum_{a'} \pi_\theta(a') \Gamma_{a'}}, \tag{12}$$

Given samples from q(a), we compute unbiased estimates of physical observables via:

$$\mathbb{E}_p[f(a)] = \sum_{a} f(a) \cdot \frac{p(a)}{q(a)} \cdot q(a) = \frac{Z'}{Z} \sum_{a} \frac{f(a)}{\pi_{\theta}(a)},\tag{13}$$

with $Z = \sum_a \Gamma_a$, $Z' = \sum_a \pi_\theta(a) \Gamma_a$. Since Γ_a cancels due to shared support, the estimator depends only on the inverse policy weight, leading to a practical self-normalized estimator:

$$\mathbb{E}_p[f(a)] \approx \sum_{i=1}^M f(a^{(i)}) \cdot \frac{1/\pi_{\theta}(a^{(i)})}{\sum_{i=1}^M 1/\pi_{\theta}(a^{(i)})}, \quad a^{(i)} \sim q(a).$$
 (14)

This guarantees unbiased estimates as long as $\pi_{\theta}(a) > 0$ for all transitions.

Trajectory-Level Correction. Beyond step-wise observables, we extend this framework to trajectory-level estimation. For a transition path $\tau = (a_1, \dots, a_T)$, the cumulative importance weight is:

$$w(\tau) = \prod_{t=1}^{T} \frac{p(a_t)}{q(a_t)} = \left(\frac{Z'}{Z}\right)^T \prod_{t=1}^{T} \frac{1}{\pi_{\theta}(a_t)}.$$
 (15)

This enables unbiased estimation of path-dependent observables—e.g., advancement factor of Cu. Although variance grows with trajectory length, it can be mitigated via entropy regularization or bounded-horizon estimation.

In summary, this formulation enables structure-aware acceleration of rare-event sampling while preserving statistical and thermodynamic consistency across both steps and trajectories—a principled fusion of learned intent and physical rigor.

5 Experiments

We evaluate the proposed method from five perspectives: correctness validation, sampling efficiency, large-scale scalability, physical visualization, and comparison with state-of-the-art baselines.

5.1 Correctness Verification

To assess physical fidelity, we evaluate the advancement factor $\zeta(t)$, which measures configurational evolution over time. Results are compared against OpenKMC with pair potentials and experimental data from Lê et al. [64] and Vincent et al. [65] at 663–773 K.

As shown in Figure 2, our method yields advancement curves that closely follow both simulation baselines and experimental measurements. At lower temperatures (e.g., 663 K), where transitions are dominated by high barriers, our model reproduces the slower configurational evolution observed experimentally. At higher temperatures (e.g., 773 K), our approach captures the rapid saturation behavior with high accuracy. These results confirm that the proposed model preserves the thermodynamic pathways and kinetics characteristic of atomic-scale diffusion processes.

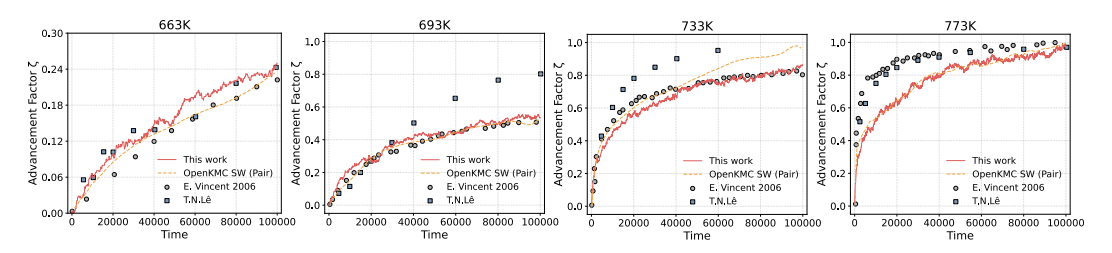


Figure 2: Advancement factor $\zeta(t)$ versus time under four thermal conditions (663 K to 773 K). Our method (red solid line) shows close agreement with OpenKMC using short-range pair potentials (orange dashed) and aligns well with experimental benchmarks from Vincent et al. [65] (black circles) and Lê et al. [64] (gray squares). The results demonstrate the physical correctness of the learned policy across a broad activation spectrum.

5.2 Sampling Efficiency

We evaluate sampling efficiency using the *Speedup Ratio*, which quantifies how many more steps a conventional KMC algorithm must take to achieve the same structural evolution as our RL-augmented method. A higher ratio indicates more efficient progression through kinetically meaningful transitions.

Across all Cu alloy systems, our method delivers substantial acceleration over conventional KMC, with the Speedup Ratio peaking at 9361x (4.02 at.% Cu, 663 K). Even in thermally activated, defect-rich regimes (5.36 at.% Cu, 773 K), it sustains over 850x speedup on average. In dilute conditions (1.34 at.% Cu), median gains remain above 1500x at 663 K and 500x at 773 K. These results highlight the method's consistent efficiency and broad applicability across diverse compositional and kinetic landscapes.

5.3 Supercomputing-Scale Simulation

We demonstrate the scalability of our method by simulating Cu alloy systems containing up to 54 billion (5.4×10^{10}) atoms, matching the problem scales previously handled only by massively parallel supercomputers such as Sunway TaihuLight. In contrast, our method executes them on a single NVIDIA A100 GPU.

Figure 4 shows the cumulative energy decrease ΔE across 10,000 steps under four Cu compositions (1.5–6.0 × 10⁻⁴ at.%). All systems exhibit smooth, monotonic relaxation, confirming the physical

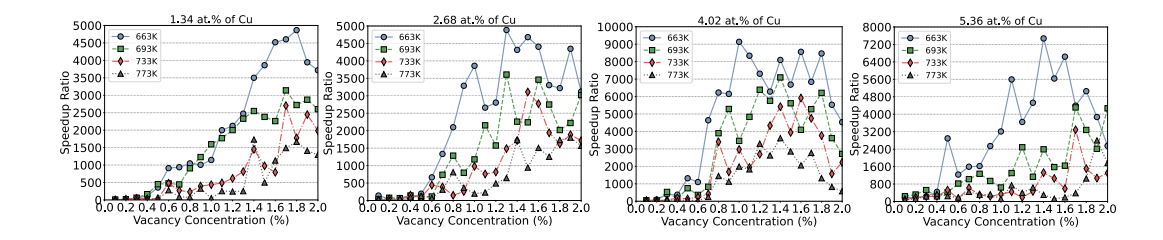


Figure 3: **Sampling acceleration across different Cu alloy systems.** Speedup Ratio is defined as the number of KMC steps required to match the structural evolution achieved by RL-based sampling. Each panel shows performance under varying vacancy concentrations for a fixed Cu composition (1.34–5.36 at.% Cu). Higher ratios reflect more efficient exploration of the configuration space. Our method maintains robust acceleration across temperature and composition regimes.

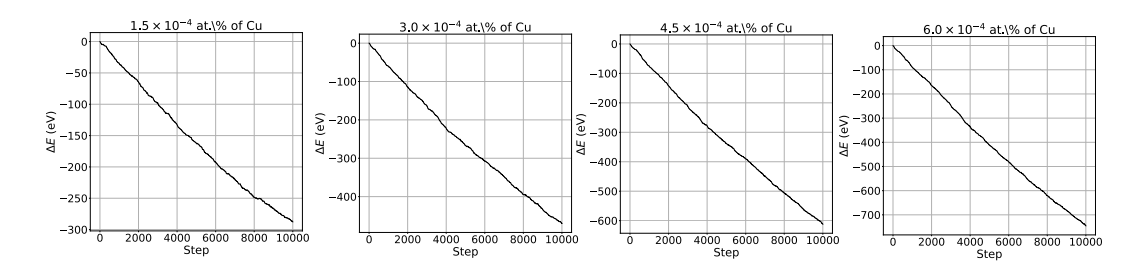


Figure 4: **Supercomputing-scale relaxation on a single GPU.** Each panel plots the cumulative system energy change ΔE over 10,000 KMC steps for increasingly concentrated Cu alloys (1.5–6.0 \times 10⁻⁴ at.%).

robustness of the learned policy under high-defect, large-scale regimes. No instability or divergence is observed, even under extreme concentrations, validating both the accuracy of the kinetic modeling and the generalizability of the policy.

To quantify resource efficiency, we compare peak memory usage against OpenKMC—the state-of-the-art conventional KMC implementation—whose baseline consumption exceeds 38.8 TB for comparable systems. As shown in Figure 5, our method consistently maintains total memory below 60GB, achieving memory efficiency gains exceeding 500×. This reduction is made through adaptive GPU-CPU memory management and redundant transition avoidance.

These results demonstrate that our system enables physically faithful simulation of previously supercomputer-only workloads using a single commodity GPU, offering a practical and efficient path to long-timescale, high-fidelity KMC at unprecedented scale.

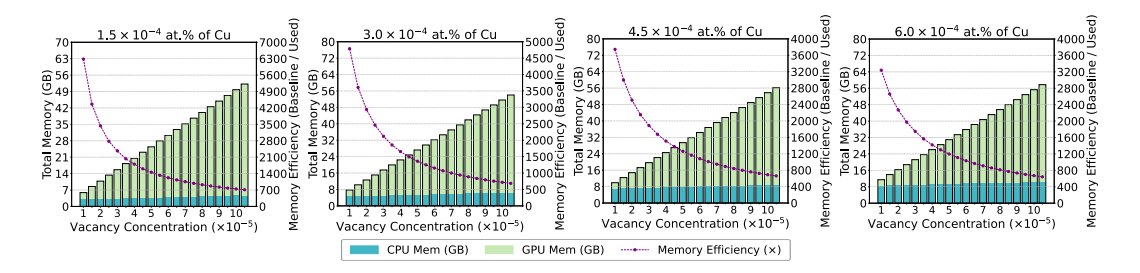


Figure 5: **Memory efficiency comparison with OpenKMC.** Each panel shows the total memory usage (CPU + GPU) across vacancy concentrations for a fixed Cu composition. Bars indicate actual peak usage of our method, while the purple dashed line denotes *Memory Efficiency*—the ratio of OpenKMC's estimated baseline memory on Sunway to ours.

5.4 Physical Visualization

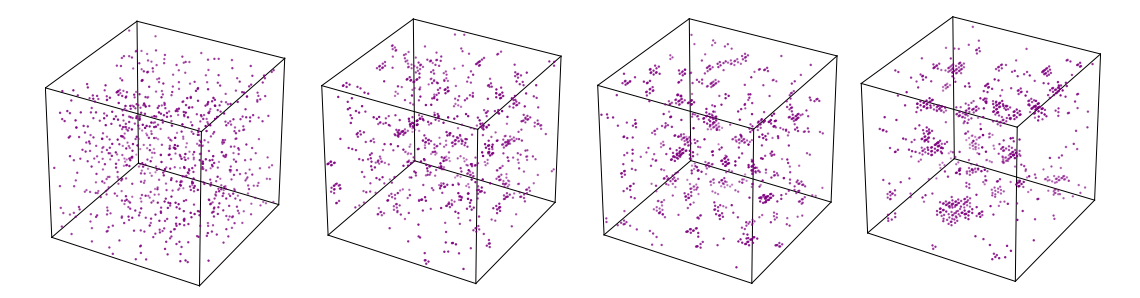


Figure 6: Cu clustering evolution in Fe–0.67 at.% Cu over 50 years. Snapshots show representative configurations at four physical time points simulated under SwarmThinkers. Starting from an initially dispersed distribution, Cu atoms progressively form and coarsen into nanoscale clusters, faithfully reproducing the thermally activated phase separation process observed in RPV steels.

Figure 6 illustrates the 50-year evolution of Cu atoms in Fe–0.67 at.% Cu, a canonical aging scenario in reactor pressure vessel (RPV) steels. The system undergoes a two-stage transformation: initial nucleation of clusters followed by long-term coarsening, matching experimentally observed phase separation behavior.

This trajectory highlights SwarmThinkers' ability to autonomously uncover physically valid pathways under dilute, high-barrier conditions, without relying on handcrafted rules or transition catalogs. Unlike conventional KMC, which often becomes trapped in metastable states, our method consistently drives the system toward thermodynamically favorable configurations, offering both predictive accuracy and interpretable structural insight.

6 Limitations and Future Work

This work introduces a scalable learning paradigm for rare-event atomistic simulation, achieving high-fidelity evolution in billion-atom systems on a single GPU. While we focus on binary alloys and single-node deployment, the underlying framework is broadly extensible toward more complex chemistries and larger computational scales.

Multi-component generalization. Our current implementation is limited to binary Cu systems. However, the agent-centric architecture is inherently species-agnostic and topology-aware, allowing seamless extension to chemically disordered or high-entropy alloys. This enables direct simulation of complex real-world materials—from radiation-tolerant steels to aerospace-grade superalloys—without relying on surrogate approximations or coarse-grained abstractions.

Distributed scalability. We have not yet implemented multi-GPU or multi-node execution. Nonetheless, the communication-free nature of agent rollouts makes the framework intrinsically parallelizable. With distributed deployment, SwarmThinkers could exceed the atomistic scale of previous supercomputer-based efforts, advancing toward trillion-atom, long-timescale simulations that resolve realistic microstructural evolution in full physical fidelity.

7 Conclusion

We introduced SwarmThinkers, a reinforcement learning framework that redefines atomic-scale simulation as a physically grounded, agent-driven decision process. By unifying physical consistency, interpretability, and scalability, SwarmThinkers enables structure-aware simulations that reason, rather than sample. It is the first system to conduct full-scale nuclear precipitations scaling to 54 billion atoms on a single GPU with less than 60GB of memory, previously possible only with supercomputers.

A Experimental Details

Table 2 summarizes the key configurations used across the four primary evaluation tasks presented in this work: correctness verification, sampling efficiency assessment, large-scale scalability testing, and physical trajectory visualization. These experiments are designed to comprehensively evaluate the accuracy, efficiency, and scalability of the proposed RL-augmented KMC framework.

In the **Correctness** task, we simulate Fe-1.34 at.% Cu systems at four temperatures (663-773 K) to validate that our model reproduces thermodynamically consistent kinetics, using advancement factor $\zeta(t)$ as a diagnostic metric. The **Sampling Efficiency** task spans a broader range of Cu compositions (1.34-5.36 at.%) under the same temperature settings to quantify acceleration over conventional KMC.

The **Scalability** task focuses on ultra-large-scale simulations with up to 54 billion atoms, evaluating both physical stability and memory performance. Here, we simulate systems with extremely dilute Cu concentrations (0.015–0.06 at.%) in a $2000 \times 3000 \times 9000$ lattice. Finally, the **Visualization** task models Cu clustering over 50 years of physical time at Fe–0.67 at.% Cu, providing interpretable atomistic trajectories that align with experimental observations in RPV steels.

All experiments share a consistent reinforcement learning architecture. Both the actor and critic networks use a 5-layer multilayer perceptron (MLP) with 256 hidden units per layer and ReLU activations. The system size remains fixed at $40 \times 40 \times 40$ for most experiments, except for the scalability benchmark. Each experiment adopts physically meaningful temperature and composition settings to stress-test the method under varying diffusion regimes.

Table 2: Summary of experimental settings across the four core evaluation tasks, including composition, temperature, system size, and RL model configurations. Each column corresponds to a distinct experiment.

Aspect	Correctness Sampling Efficiency	Scalability	Visualization		
Cu composition	1.34 at.% 1.34 / 2.68 / 4.02 / 5.36 at.%	\mid 1.5 / 3.0 / 4.5 / 6.0 $\times 10^{-4}$ at.% \mid	0.67 at.%		
Temperature (K)	663 / 693 / 733 / 773	663	663		
System scale	$40 \times 40 \times 40$	$ \hspace{0.2in}2000\times3000\times9000\hspace{0.2in} $	$40 \times 40 \times 40$		
Actor network	5-layer MLP: [256, 256, 256, 256, 256], ReLU				
Critic network	5-layer MLP: [256, 256, 256, 256], ReLU				
Purpose	Validate $\zeta(t)$ Measure Speedup Ratio	Memory and compute scaling	Cu clustering over 50 years		

Table 3: Summary of the reinforcement learning training configuration used consistently across all experiments. Parameters are grouped into two categories: RL strategy (e.g., discounting, advantage estimation, and loss weighting) and optimization/execution (e.g., optimizer choice, batch size, and training schedule). These settings follow standard PPO practices while balancing training stability and sample efficiency.

RL Strategy	Value	Optimization / Execution	Value
Algorithm	PPO	Optimizer	Adam
Discount factor γ	0.99	Learning rate	5×10^{-4}
GAE λ	0.95	Mini-batch size	256
Entropy coefficient	0.01	PPO epochs	10
Value loss coefficient	0.5	Grad clip (norm)	0.2
Episode length	2048	Training time	24 hr

B Training Configuration

All reinforcement learning experiments are conducted using Proximal Policy Optimization (PPO), chosen for its stability and efficiency in on-policy policy gradient settings. Table 3 summarizes the training configuration adopted uniformly across all tasks. The hyperparameters are grouped into two functional categories: RL strategy and optimization/runtime settings.

In the RL strategy group, we use a discount factor of $\gamma=0.99$ and generalized advantage estimation (GAE) with $\lambda=0.95$ to stabilize learning and reduce variance. The entropy coefficient and value loss coefficient are set to 0.01 and 0.5, respectively, encouraging sufficient exploration while maintaining value accuracy.

Optimization is performed using the Adam optimizer with a learning rate of 5×10^{-4} . Each policy update involves 10 PPO epochs with a mini-batch size of 256 and gradient clipping at a maximum norm of 0.2 to ensure training stability. Episodes consist of 2048 environment steps, and A typical training run consists of 100,000 episodes and completes within 24 hours.

To ensure efficiency and robustness during training, all policy networks are trained on small lattice environments with dimensions $10 \times 10 \times 10$. This design choice allows rapid sampling and policy iteration without compromising the learned policy's ability to generalize. Once trained, the learned policy is directly transferred to larger physical systems (up to 5.4×10^{10} atoms) without any additional fine-tuning, demonstrating strong scalability and transferability.

References

- [1] Christophe Domain and Charlotte S. Becquart. *Object Kinetic Monte Carlo (OKMC): A Coarse-Grained Approach to Radiation Damage*, pages 1–26. Springer International Publishing, Cham, 2019.
- [2] Mie Andersen, Chiara Panosetti, and Karsten Reuter. A practical guide to surface kinetic monte carlo simulations. *Frontiers in Chemistry*, Volume 7 2019, 2019.
- [3] Y. Gao, Y. Zhang, D. Schwen, E. Martinez, and I. J. Beyerlein. Theoretical prediction and atomic kinetic monte carlo simulations of void superlattice self-organization under irradiation. *Scientific Reports*, 8(1):6629, 2018.
- [4] Enrique Martínez, María José Caturla, and Jaime Marian. *DFT-Parameterized Object Kinetic Monte Carlo Simulations of Radiation Damage*, pages 2457–2488. Springer International Publishing, Cham, 2020.
- [5] Chaitanya Deo, Elton Chen, and Remi Dingreville. Atomistic modeling of radiation damage in crystalline materials. *Modelling and Simulation in Materials Science and Engineering*, 30, 12 2021.
- [6] A. Roy, G. Nandipati, A. M. Casella, C. H. Henager, and W. Setyawan. A review of displacement cascade simulations using molecular dynamics emphasizing interatomic potentials for tpbar components. *npj Materials Degradation*, 9(1):1, 2025.
- [7] M. Pineda and M. Stamatakis. Kinetic monte carlo simulations for heterogeneous catalysis: Fundamentals, current status, and challenges. *The Journal of Chemical Physics*, 156(12):120902, 03 2022.
- [8] Animesh Chatterjee and Dionisios G. Vlachos. An overview of spatial microscopic and accelerated kinetic monte carlo methods. *Journal of Computer-Aided Materials Design*, 14(2):253–308, 2007.
- [9] Haixuan Xu, Roger E. Stoller, Laurent K. Béland, and Yuri N. Osetsky. Self-evolving atomistic kinetic monte carlo simulations of defects in materials. *Computational Materials Science*, 100:135–143, 2015. Special Issue on Advanced Simulation Methods.
- [10] A. P. J. Jansen. An introduction to monte carlo simulations of surface reactions, 2003.
- [11] Graeme Henkelman and Hannes Jónsson. Long time scale kinetic monte carlo simulations without lattice approximation and predefined event table. *The Journal of Chemical Physics*, 115(21):9657–9666, 12 2001.
- [12] Aleksandar Donev, Vasily V. Bulatov, Tomas Oppelstrup, George H. Gilmer, Babak Sadigh, and Malvin H. Kalos. A first-passage kinetic monte carlo algorithm for complex diffusion–reaction systems. *Journal of Computational Physics*, 229(9):3214–3236, May 2010.
- [13] Atsushi Ito, Jesús J. Ramos, and Noriyoshi Nakajima. Ellipticity of axisymmetric equilibria with flow and pressure anisotropy in single-fluid and hall magnetohydrodynamics. *Physics of Plasmas*, 14(6):062502, 06 2007.
- [14] Rosalind J. Allen, Daan Frenkel, and Pieter Rein ten Wolde. Simulating rare events in equilibrium or nonequilibrium stochastic systems. *The Journal of Chemical Physics*, 124(2), January 2006.
- [15] Carlos Pérez-Espigares and Pablo I. Hurtado. Sampling rare events across dynamical phase transitions. *Chaos: An Interdisciplinary Journal of Nonlinear Science*, 29(8), August 2019.
- [16] Robin Shannon and David R. Glowacki. A simple "boxed molecular kinetics" approach to accelerate rare events in the stochastic kinetic master equation. *The Journal of Physical Chemistry A*, 122(6):1531–1541, January 2018.
- [17] Konstantinos G. Papakonstantinou, Hamed Nikbakht, and Elsayed Eshra. Hamiltonian mcmc methods for estimating rare events probabilities in high-dimensional problems, 2023.

- [18] Stavros Ntioudis, James P. Ewen, Daniele Dini, and C. Heath Turner. A hybrid off-lattice kinetic monte carlo/molecular dynamics method for amorphous thin film growth. *Computational Materials Science*, 229:112421, 2023.
- [19] J. Torre, Jean-Louis Bocquet, N.V Doan, Erwan Adam, and A. Barbu. Jerk, an event-based kinetic monte carlo model to predict microstructure evolution of materials under irradiation. *Philosophical Magazine*, 85:549–558, 02 2005.
- [20] Daniel Mason, Toby Hudson, and A. Sutton. Fast recall of state-history in kinetic monte carlo simulations utilizing the zobrist key. *Computer Physics Communications*, 165:37–48, 01 2005.
- [21] Tomas Oppelstrup, Vasily V. Bulatov, Aleksandar Donev, Malvin H. Kalos, George H. Gilmer, and Babak Sadigh. First-passage kinetic monte carlo method. *Physical Review E*, 80(6), December 2009.
- [22] J. D. Muñoz, M. A. Novotny, and S. J. Mitchell. Rejection-free monte carlo algorithms for models with continuous degrees of freedom. *Physical Review E*, 67(2), February 2003.
- [23] Jin Yang and William S. Hlavacek. Rejection-free kinetic monte carlo simulation of multivalent biomolecular interactions, 2010.
- [24] Hamza Ruzayqat. A rejection scheme for off-lattice kinetic monte carlo simulations, 10 2017.
- [25] Alexander Slepoy, Aidan Thompson, and Steven Plimpton. A constant-time kinetic monte carlo algorithm for simulation of large biochemical reaction networks. *The Journal of chemical physics*, 128:205101, 06 2008.
- [26] Qingyi Lin, Chuang Zhang, Xuhui Meng, and Zhaoli Guo. Monte carlo physics-informed neural networks for multiscale heat conduction via phonon boltzmann transport equation, 2024.
- [27] N. Castin, L. Messina, C. Domain, R. C. Pasianot, and P. Olsson. Improved atomistic monte carlo models based on ab-initio-trained neural networks: Application to fecu and fecr alloys. *Phys. Rev. B*, 95:214117, Jun 2017.
- [28] Kun Li, Honghui Shang, Yunquan Zhang, Shigang Li, Baodong Wu, Dong Wang, Libo Zhang, Fang Li, Dexun Chen, and Zhiqiang Wei. Openkmc: a kmc design for hundred-billion-atom simulation using millions of cores on sunway taihulight. In *Proceedings of the International Conference for High Performance Computing, Networking, Storage and Analysis*, SC '19, New York, NY, USA, 2019. Association for Computing Machinery.
- [29] Arthur F Voter. Hyperdynamics: Accelerated molecular dynamics of infrequent events. *Physical Review Letters*, 78(20):3908, 1997.
- [30] Richard J Zamora, Arthur F Voter, Danny Perez, Nandakishore Santhi, Susan M Mniszewski, Sunil Thulasidasan, and Stephan J Eidenbenz. Discrete event performance prediction of speculatively parallel temperature-accelerated dynamics. *Simulation*, 92(12):1065–1086, December 2016.
- [31] Yen Ting Lin, Song Feng, and William S. Hlavacek. Scaling methods for accelerating kinetic monte carlo simulations of chemical reaction networks. *The Journal of Chemical Physics*, 150(24):244101, 2019.
- [32] Zhirong Liu. Accelerating kinetics with time-reversal path sampling, 2023.
- [33] Hao Tang, Boning Li, Yixuan Song, Mengren Liu, Haowei Xu, Guoqing Wang, Heejung Chung, and Ju Li. Reinforcement learning-guided long-timescale simulation of hydrogen transport in metals, 2023.
- [34] Troels Arnfred Bojesen. Policy-guided monte carlo: Reinforcement-learning markov chain dynamics. *Physical Review E*, 98(6), December 2018.
- [35] T. S. Rahman et al. Atomistic studies of thin film growth. arXiv preprint cond-mat/0501317, 2005.

- [36] P. Kratzer. Monte carlo and kinetic monte carlo methods. arXiv preprint arXiv:0904.2556, 2009.
- [37] J. Yang, M. I. Monine, J. R. Faeder, and W. S. Hlavacek. Kinetic monte carlo method for rule-based modeling of biochemical networks. *Physical Review E*, 78(3):031910, 2008.
- [38] D. T. Gillespie. Stochastic simulation of chemical kinetics. Annual Review of Physical Chemistry, 58:35–55, 2007.
- [39] Zhucong Xi, Louis Hector, Amit Misra, and Liang Qi. Kinetic monte carlo simulations of solute clustering during quenching and aging of al-mg-zn alloys. *Acta Materialia*, 269:119795, 03 2024.
- [40] Brian Douglas Hehr. Analysys of defect clustering in semiconductors using kinetic monte carlo methods. Sandia National Lab. (SNL-NM), Albuquerque, NM (United States), 07 2013.
- [41] C. S. Becquart and F. Soisson. Monte carlo simulations of precipitation under irradiation. In *Handbook of Mechanics of Materials*, pages 703–731. Springer, 2019.
- [42] C. S. Becquart and B. D. Wirth. Kinetic monte carlo simulations of irradiation effects. In *Comprehensive Nuclear Materials*, pages 393–410. Elsevier, 2012.
- [43] R. A. Miron and K. A. Fichthorn. Accelerated molecular dynamics with the parallel replica method. *The Journal of Chemical Physics*, 119(12):6210–6216, 2003.
- [44] Animesh Chatterjee and Arthur F Voter. Accurate acceleration of kinetic monte carlo simulations through the modification of rate constants. *The Journal of Chemical Physics*, 132(19):194101, 2010.
- [45] Arthur F Voter. Parallel replica method for dynamics of infrequent events. *Physical Review B*, 57(22):R13985, 1998.
- [46] Danny Perez, Blas P. Uberuaga, Yunsic Shim, Jacques G. Amar, and Arthur F. Voter. Accelerated molecular dynamics methods: Introduction and recent developments. *Annual Reports in Computational Chemistry*, 5:79–98, 2009.
- [47] Gideon Simpson and Mitchell Luskin. Numerical analysis of parallel replica dynamics. *Multiscale Modeling & Simulation*, 9(2):593–606, 2011.
- [48] Graeme Henkelman, Blas P. Uberuaga, and Hannes Jónsson. A climbing image nudged elastic band method for finding saddle points and minimum energy paths. *The Journal of Chemical Physics*, 113(22):9901–9904, 2000.
- [49] Lei Xu and Graeme Henkelman. Adaptive kinetic monte carlo for first-principles accelerated dynamics. *The Journal of Chemical Physics*, 129(11):114104, 2008.
- [50] J. A. Mitchell, F. Abdeljawad, C. C. Battaile, et al. Parallel simulation via spparks of on-lattice kinetic and metropolis monte carlo models for materials processing. *Modelling and Simulation* in *Materials Science and Engineering*, 31(5):055001, 2023.
- [51] Haoya Shang et al. Tensorkmc: Kinetic monte carlo simulation of 50 trillion atoms with tensorflow. In SC '21: Proceedings of the International Conference for High Performance Computing, Networking, Storage and Analysis, pages 1–14. IEEE, 2021.
- [52] Jyri Kimari, Ville Jansson, Simon Vigonski, Ekaterina Baibuz, Roberto Domingos, Vahur Zadin, and Flyura Djurabekova. Application of artificial neural networks for rigid lattice kinetic monte carlo studies of cu surface diffusion. *Computational Materials Science*, 183:109789, 2020.
- [53] J. R. Gonzalez and D. G. Vlachos. Machine learning-based kinetic monte carlo simulations. *AIChE Journal*, 65(3):1006–1016, 2019.
- [54] Patrick Reiser, Marlen Neubert, André Eberhard, Luca Torresi, Chen Zhou, Chen Shao, Houssam Metni, Clint van Hoesel, Henrik Schopmans, Timo Sommer, and Pascal Friederich. Graph neural networks for materials science and chemistry, 2022.

- [55] Kamal Choudhary and Brian DeCost. Atomistic line graph neural network for improved materials property predictions. npj Computational Materials, 7(1):185, 2021.
- [56] Victor Fung, Jie Zhang, Enrique Juarez, and Bobby G. Sumpter. Benchmarking graph neural networks for materials chemistry. *npj Computational Materials*, 7(1):84, 2021.
- [57] Wang Zijun, Du Xiaoming, Li Tianfu, Sun Kai, Tong Xuezhu, Li Meijuan, Liu Rongdeng, Liu Yuntao, and Chen Dongfeng. Investigation of cu-enriched precipitates in thermally aged fe-cu and fe-cu-ni model alloys. *Journal of Nuclear Materials*, 562:153601, 02 2022.
- [58] Senlin Cui, Mahmood Mamivand, and Dane Morgan. Simulation of cu precipitation in fe-cu dilute alloys with cluster mobility. *Materials & Design*, 191:108574, 02 2020.
- [59] Guojun Wei, Chenglong Wang, Xingwang Yang, Zhenfeng Tong, and Wenwang Wu. Non-hardening embrittlement mechanism of pressure vessel steel ni-cr-mo-v welds during thermal aging. *Advances in Mechanical Engineering*, 12:168781402090456, 02 2020.
- [60] Te Zhu, Haibiao Wu, Xingzhong Cao, Shuoxue Jin, Peng Zhang, Ainong Xiao, and Baoyi Wang. Formation and recovery of cu precipitates in fe—cu model alloys under varying heat treatment. *physica status solidi* (a), 214(5):1600785, 2017.
- [61] Xian-Ming Bai, Huibin Ke, Yongfeng Zhang, and Benjamin Spencer. Modeling copper precipitation hardening and embrittlement in a dilute fe-0.3at. *Journal of Nuclear Materials*, 495, 09 2017.
- [62] Qigui Yang and Par Olsson. Identification and evolution of ultrafine precipitates in fe-cu alloys by first-principles modeling of positron annihilation. *Acta Materialia*, 242, 10 2022.
- [63] Frédéric Christien and A. Barbu. Modelling of copper precipitation in iron during thermal aging and irradiation. *Journal of Nuclear Materials*, 324:90–96, 01 2004.
- [64] T. N. Lê, A. Barbu, D. Liu, and F. Maury. Precipitation kinetics of dilute fecu and fecumn alloys subjected to electron irradiation. *Scripta Metallurgica et Materialia*, 26(5):771–776, 1992.
- [65] E. Vincent, C. S. Becquart, and C. Domain. Solute interaction with point defects in α -fe during thermal ageing: A combined *ab initio* and atomic kinetic monte carlo approach. *Journal of Nuclear Materials*, 351(1–3):88–99, 2006.

NeurIPS Paper Checklist

1. Claims

Question: Do the main claims made in the abstract and introduction accurately reflect the paper's contributions and scope?

Answer: [Yes]

Justification: The abstract and introduction accurately capture the paper's key innovations—including the agent-based formulation, reweighting mechanism, CTDE training, and large-scale benchmark results. All stated contributions are later substantiated with technical details and quantitative evidence.

Guidelines:

- The answer NA means that the abstract and introduction do not include the claims made in the paper.
- The abstract and/or introduction should clearly state the claims made, including the contributions made in the paper and important assumptions and limitations. A No or NA answer to this question will not be perceived well by the reviewers.
- The claims made should match theoretical and experimental results, and reflect how much the results can be expected to generalize to other settings.
- It is fine to include aspirational goals as motivation as long as it is clear that these goals
 are not attained by the paper.

2. Limitations

Question: Does the paper discuss the limitations of the work performed by the authors?

Answer: [Yes]

Justification: Yes, please see Sec. 6 for limitations.

Guidelines:

- The answer NA means that the paper has no limitation while the answer No means that the paper has limitations, but those are not discussed in the paper.
- The authors are encouraged to create a separate "Limitations" section in their paper.
- The paper should point out any strong assumptions and how robust the results are to violations of these assumptions (e.g., independence assumptions, noiseless settings, model well-specification, asymptotic approximations only holding locally). The authors should reflect on how these assumptions might be violated in practice and what the implications would be.
- The authors should reflect on the scope of the claims made, e.g., if the approach was only tested on a few datasets or with a few runs. In general, empirical results often depend on implicit assumptions, which should be articulated.
- The authors should reflect on the factors that influence the performance of the approach. For example, a facial recognition algorithm may perform poorly when image resolution is low or images are taken in low lighting. Or a speech-to-text system might not be used reliably to provide closed captions for online lectures because it fails to handle technical jargon.
- The authors should discuss the computational efficiency of the proposed algorithms and how they scale with dataset size.
- If applicable, the authors should discuss possible limitations of their approach to address problems of privacy and fairness.
- While the authors might fear that complete honesty about limitations might be used by reviewers as grounds for rejection, a worse outcome might be that reviewers discover limitations that aren't acknowledged in the paper. The authors should use their best judgment and recognize that individual actions in favor of transparency play an important role in developing norms that preserve the integrity of the community. Reviewers will be specifically instructed to not penalize honesty concerning limitations.

3. Theory assumptions and proofs

Question: For each theoretical result, does the paper provide the full set of assumptions and a complete (and correct) proof?

Answer: [Yes]

Justification: Yes, the proof of statistical consistency is provided in Sec. 4.3.

Guidelines:

- The answer NA means that the paper does not include theoretical results.
- All the theorems, formulas, and proofs in the paper should be numbered and crossreferenced.
- All assumptions should be clearly stated or referenced in the statement of any theorems.
- The proofs can either appear in the main paper or the supplemental material, but if they appear in the supplemental material, the authors are encouraged to provide a short proof sketch to provide intuition.
- Inversely, any informal proof provided in the core of the paper should be complemented by formal proofs provided in appendix or supplemental material.
- Theorems and Lemmas that the proof relies upon should be properly referenced.

4. Experimental result reproducibility

Question: Does the paper fully disclose all the information needed to reproduce the main experimental results of the paper to the extent that it affects the main claims and/or conclusions of the paper (regardless of whether the code and data are provided or not)?

Answer: [Yes]

Justification: We describe the simulation environment, physical settings in Sec. 5 and Sec. A, and the full structure of our reinforcement learning algorithm in Sec. 4.2 and Sec. B.

Guidelines:

- The answer NA means that the paper does not include experiments.
- If the paper includes experiments, a No answer to this question will not be perceived well by the reviewers: Making the paper reproducible is important, regardless of whether the code and data are provided or not.
- If the contribution is a dataset and/or model, the authors should describe the steps taken to make their results reproducible or verifiable.
- Depending on the contribution, reproducibility can be accomplished in various ways. For example, if the contribution is a novel architecture, describing the architecture fully might suffice, or if the contribution is a specific model and empirical evaluation, it may be necessary to either make it possible for others to replicate the model with the same dataset, or provide access to the model. In general, releasing code and data is often one good way to accomplish this, but reproducibility can also be provided via detailed instructions for how to replicate the results, access to a hosted model (e.g., in the case of a large language model), releasing of a model checkpoint, or other means that are appropriate to the research performed.
- While NeurIPS does not require releasing code, the conference does require all submissions to provide some reasonable avenue for reproducibility, which may depend on the nature of the contribution. For example
- (a) If the contribution is primarily a new algorithm, the paper should make it clear how to reproduce that algorithm.
- (b) If the contribution is primarily a new model architecture, the paper should describe the architecture clearly and fully.
- (c) If the contribution is a new model (e.g., a large language model), then there should either be a way to access this model for reproducing the results or a way to reproduce the model (e.g., with an open-source dataset or instructions for how to construct the dataset).
- (d) We recognize that reproducibility may be tricky in some cases, in which case authors are welcome to describe the particular way they provide for reproducibility. In the case of closed-source models, it may be that access to the model is limited in some way (e.g., to registered users), but it should be possible for other researchers to have some path to reproducing or verifying the results.

5. Open access to data and code

Question: Does the paper provide open access to the data and code, with sufficient instructions to faithfully reproduce the main experimental results, as described in supplemental material?

Answer: [Yes]

Justification: The full source code, along with detailed instructions for reproducing all experiments and figures, will be released upon paper acceptance. We are actively preparing the repository to ensure clarity and usability for the community.

Guidelines:

- The answer NA means that paper does not include experiments requiring code.
- Please see the NeurIPS code and data submission guidelines (https://nips.cc/public/guides/CodeSubmissionPolicy) for more details.
- While we encourage the release of code and data, we understand that this might not be possible, so "No" is an acceptable answer. Papers cannot be rejected simply for not including code, unless this is central to the contribution (e.g., for a new open-source benchmark).
- The instructions should contain the exact command and environment needed to run to reproduce the results. See the NeurIPS code and data submission guidelines (https://nips.cc/public/guides/CodeSubmissionPolicy) for more details.
- The authors should provide instructions on data access and preparation, including how to access the raw data, preprocessed data, intermediate data, and generated data, etc.
- The authors should provide scripts to reproduce all experimental results for the new proposed method and baselines. If only a subset of experiments are reproducible, they should state which ones are omitted from the script and why.
- At submission time, to preserve anonymity, the authors should release anonymized versions (if applicable).
- Providing as much information as possible in supplemental material (appended to the paper) is recommended, but including URLs to data and code is permitted.

6. Experimental setting/details

Question: Does the paper specify all the training and test details (e.g., data splits, hyper-parameters, how they were chosen, type of optimizer, etc.) necessary to understand the results?

Answer: [Yes]

Justification: The Experimental setting is discribed in Sec. A and Sec. B.

Guidelines:

- The answer NA means that the paper does not include experiments.
- The experimental setting should be presented in the core of the paper to a level of detail that is necessary to appreciate the results and make sense of them.
- The full details can be provided either with the code, in appendix, or as supplemental material.

7. Experiment statistical significance

Question: Does the paper report error bars suitably and correctly defined or other appropriate information about the statistical significance of the experiments?

Answer: [No]

Justification: Due to computational constraints, we do not report error bars. As noted in Sec. 5.3, each experiment involves billion-atom simulations at supercomputer scale, making repeated runs prohibitively expensive.

Guidelines:

- The answer NA means that the paper does not include experiments.
- The authors should answer "Yes" if the results are accompanied by error bars, confidence intervals, or statistical significance tests, at least for the experiments that support the main claims of the paper.

- The factors of variability that the error bars are capturing should be clearly stated (for example, train/test split, initialization, random drawing of some parameter, or overall run with given experimental conditions).
- The method for calculating the error bars should be explained (closed form formula, call to a library function, bootstrap, etc.)
- The assumptions made should be given (e.g., Normally distributed errors).
- It should be clear whether the error bar is the standard deviation or the standard error
 of the mean.
- It is OK to report 1-sigma error bars, but one should state it. The authors should preferably report a 2-sigma error bar than state that they have a 96% CI, if the hypothesis of Normality of errors is not verified.
- For asymmetric distributions, the authors should be careful not to show in tables or figures symmetric error bars that would yield results that are out of range (e.g. negative error rates).
- If error bars are reported in tables or plots, The authors should explain in the text how they were calculated and reference the corresponding figures or tables in the text.

8. Experiments compute resources

Question: For each experiment, does the paper provide sufficient information on the computer resources (type of compute workers, memory, time of execution) needed to reproduce the experiments?

Answer: [Yes]

Justification: All experiments were conducted on a single NVIDIA A100 GPU. We report detailed memory usage (CPU and GPU) for experiment in Fig. 5, and specify execution settings including atom counts, vacancy concentrations, and simulation steps in Sec. 5.

Guidelines:

- The answer NA means that the paper does not include experiments.
- The paper should indicate the type of compute workers CPU or GPU, internal cluster, or cloud provider, including relevant memory and storage.
- The paper should provide the amount of compute required for each of the individual experimental runs as well as estimate the total compute.
- The paper should disclose whether the full research project required more compute than the experiments reported in the paper (e.g., preliminary or failed experiments that didn't make it into the paper).

9. Code of ethics

Question: Does the research conducted in the paper conform, in every respect, with the NeurIPS Code of Ethics https://neurips.cc/public/EthicsGuidelines?

Answer: [Yes]

Justification: This work involves atomistic simulations using reinforcement learning and does not involve human subjects, personal data, or environmental impact. All methods, assumptions, and limitations are transparently reported in accordance with the NeurIPS Code of Ethics.

Guidelines:

- The answer NA means that the authors have not reviewed the NeurIPS Code of Ethics.
- If the authors answer No, they should explain the special circumstances that require a
 deviation from the Code of Ethics.
- The authors should make sure to preserve anonymity (e.g., if there is a special consideration due to laws or regulations in their jurisdiction).

10. Broader impacts

Question: Does the paper discuss both potential positive societal impacts and negative societal impacts of the work performed?

Answer: [Yes]

Justification: This work facilitates efficient, high-fidelity simulation of complex materials, potentially accelerating advances in energy, aerospace, and semiconductor technologies. It lowers the barrier to large-scale modeling, making atomic-level simulation more broadly accessible.

- The answer NA means that there is no societal impact of the work performed.
- If the authors answer NA or No, they should explain why their work has no societal impact or why the paper does not address societal impact.
- Examples of negative societal impacts include potential malicious or unintended uses (e.g., disinformation, generating fake profiles, surveillance), fairness considerations (e.g., deployment of technologies that could make decisions that unfairly impact specific groups), privacy considerations, and security considerations.
- The conference expects that many papers will be foundational research and not tied to particular applications, let alone deployments. However, if there is a direct path to any negative applications, the authors should point it out. For example, it is legitimate to point out that an improvement in the quality of generative models could be used to generate deepfakes for disinformation. On the other hand, it is not needed to point out that a generic algorithm for optimizing neural networks could enable people to train models that generate Deepfakes faster.
- The authors should consider possible harms that could arise when the technology is being used as intended and functioning correctly, harms that could arise when the technology is being used as intended but gives incorrect results, and harms following from (intentional or unintentional) misuse of the technology.
- If there are negative societal impacts, the authors could also discuss possible mitigation strategies (e.g., gated release of models, providing defenses in addition to attacks, mechanisms for monitoring misuse, mechanisms to monitor how a system learns from feedback over time, improving the efficiency and accessibility of ML).

11. Safeguards

Question: Does the paper describe safeguards that have been put in place for responsible release of data or models that have a high risk for misuse (e.g., pretrained language models, image generators, or scraped datasets)?

Answer: [NA]

Justification: This work does not involve pretrained language models, generative image systems, or large-scale scraped datasets. It presents a reinforcement learning framework for atomistic simulation, which poses minimal risk of misuse.

Guidelines:

- The answer NA means that the paper poses no such risks.
- Released models that have a high risk for misuse or dual-use should be released with
 necessary safeguards to allow for controlled use of the model, for example by requiring
 that users adhere to usage guidelines or restrictions to access the model or implementing
 safety filters.
- Datasets that have been scraped from the Internet could pose safety risks. The authors should describe how they avoided releasing unsafe images.
- We recognize that providing effective safeguards is challenging, and many papers do
 not require this, but we encourage authors to take this into account and make a best
 faith effort.

12. Licenses for existing assets

Question: Are the creators or original owners of assets (e.g., code, data, models), used in the paper, properly credited and are the license and terms of use explicitly mentioned and properly respected?

Answer: [Yes]

Justification: All third-party assets used in this work—including baseline code, simulation environments, and referenced datasets—are properly cited in the paper. Their licenses and terms of use have been fully respected.

Guidelines:

- The answer NA means that the paper does not use existing assets.
- The authors should cite the original paper that produced the code package or dataset.
- The authors should state which version of the asset is used and, if possible, include a URL.
- The name of the license (e.g., CC-BY 4.0) should be included for each asset.
- For scraped data from a particular source (e.g., website), the copyright and terms of service of that source should be provided.
- If assets are released, the license, copyright information, and terms of use in the package should be provided. For popular datasets, paperswithcode.com/datasets has curated licenses for some datasets. Their licensing guide can help determine the license of a dataset.
- For existing datasets that are re-packaged, both the original license and the license of the derived asset (if it has changed) should be provided.
- If this information is not available online, the authors are encouraged to reach out to the asset's creators.

13. New assets

Ouestion: Are new assets introduced in the paper well documented and is the documentation provided alongside the assets?

Answer: [Yes]

Justification: We introduce a new simulation and learning framework for large-scale atomistic modeling. While the code and assets are not yet publicly released, we plan to opensource them upon acceptance. Comprehensive documentation and usage instructions will be provided to ensure accessibility and reproducibility.

- The answer NA means that the paper does not release new assets.
- · Researchers should communicate the details of the dataset/code/model as part of their submissions via structured templates. This includes details about training, license, limitations, etc.
- The paper should discuss whether and how consent was obtained from people whose asset is used.
- At submission time, remember to anonymize your assets (if applicable). You can either create an anonymized URL or include an anonymized zip file.

14. Crowdsourcing and research with human subjects

Question: For crowdsourcing experiments and research with human subjects, does the paper include the full text of instructions given to participants and screenshots, if applicable, as well as details about compensation (if any)?

Answer: [NA]

Justification: This work does not involve crowdsourcing or research with human subjects.

Guidelines:

- The answer NA means that the paper does not involve crowdsourcing nor research with human subjects.
- Including this information in the supplemental material is fine, but if the main contribution of the paper involves human subjects, then as much detail as possible should be included in the main paper.
- According to the NeurIPS Code of Ethics, workers involved in data collection, curation, or other labor should be paid at least the minimum wage in the country of the data

15. Institutional review board (IRB) approvals or equivalent for research with human subjects

Ouestion: Does the paper describe potential risks incurred by study participants, whether such risks were disclosed to the subjects, and whether Institutional Review Board (IRB) approvals (or an equivalent approval/review based on the requirements of your country or institution) were obtained?

Answer: [NA]

Justification: This work does not involve research with human subjects and therefore does not require IRB or equivalent review.

Guidelines:

- The answer NA means that the paper does not involve crowdsourcing nor research with human subjects.
- Depending on the country in which research is conducted, IRB approval (or equivalent) may be required for any human subjects research. If you obtained IRB approval, you should clearly state this in the paper.
- We recognize that the procedures for this may vary significantly between institutions and locations, and we expect authors to adhere to the NeurIPS Code of Ethics and the guidelines for their institution.
- For initial submissions, do not include any information that would break anonymity (if applicable), such as the institution conducting the review.

16. Declaration of LLM usage

Question: Does the paper describe the usage of LLMs if it is an important, original, or non-standard component of the core methods in this research? Note that if the LLM is used only for writing, editing, or formatting purposes and does not impact the core methodology, scientific rigorousness, or originality of the research, declaration is not required.

Answer: [NA]

Justification: This work does not involve the use of large language models in the development of core methods.

Guidelines:

- The answer NA means that the core method development in this research does not involve LLMs as any important, original, or non-standard components.
- Please refer to our LLM policy (https://neurips.cc/Conferences/2025/LLM) for what should or should not be described.